# Supramolecular Nanovalves Controlled by Proton Abstraction and Competitive Binding

Ken C.-F. Leung,[†] Thoi D. Nguyen,[‡] J. Fraser Stoddart,* and Jeffrey I. Zink*

*California NanoSystems Institute and Department of Chemistry and Biochemistry, University of California, Los Angeles, 405 Hilgard Avenue, Los Angeles, California 90095-1569*

*Received July 19, 2006. Revised Manuscript Received August 24, 2006*

A functional integrated nanosystem for trapping and releasing molecules under deliberate control is prepared. The openings to nanosized pores in silica particles are regulated by gatekeeper supermolecules that are controlled by pH stimulation and competitive binding. Controlled release of fluorescent probe molecules is demonstrated using (i) organic bases, (ii) fluorodialkylammonium ions, and (iii) metal ions as actuators. The rate of the release of the probe molecules depends on the size of the base, the dimension of the probe molecules, and the binding affinity of the metal/fluorodialkylammonium cations employed.

## Introduction

Trapping and releasing molecules under deliberate control from nanoscale containers is an important challenge for applications in fluidics, sensors, and controlled drug release. Functional integrated systems must be designed in which stable and inert containers for the trapped molecules are functionalized with appropriate moving parts that can either act as gatekeepers at the entrances to the containers or change the effective inner diameters of the containers. Several categories of molecules with movable components have been attached to mesoporous silica and shown to be able to regulate molecular transport into and out of the functional material.[1,2] The control (or actuator) of the transport has involved, for the most part, simple types of chemical changes driven by photons or electrons. For example, azobenzene derivatives that undergo cis−trans photoisomerization inside the pores of mesostructured silica films have been used[3] to photoregulate mass transport through the pores. These materials take advantage of the optical transparency of the silica, as well as its chemical and mechanical stabilities. Electrons (redox chemistry) have also been employed[4,5] to control access and egress of molecules to and from the pores. Cadmium sulfide nanoparticles that are chemically labile as a result of the reversibility of the thiol/disulfide redox process have been used[4] as gatekeepers to control the release of drugs. Recently, we have reported[5] that pseudorotaxanes and bistable rotaxanes, controlled by redox processes, act as the actuators of nanovalves. These examples are based on large amplitude molecular motions controlled by an external "power supply". Alternative methods for controlled release, including dimerizations[6]—for example, between coumarin derivatives—and size or shape changes of polymers,[7] have also been studied.

For future nanovalve applications, it is necessary to develop activation methodologies that utilize conditions specific to the application: light, heat, redox, and other chemical stimuli are all being investigated. Recently, we reported[8] that a supramolecular system based on the dibenzo-[24]crown-8 (DB24C8)/dialkylammonium ion pseudorotaxane functions as the moving parts of nanovalves. Abstraction of protons from the dialkylammonium moieties by action of a base (such as triethylamine) switches off the hydrogen bonding between the dialkylammonium ion and the DB24C8 rings, leading to dissociation of the rings and opening of the nanovalves. This system also offers an alternative method of activation based on the competitive binding of the DB24C8 ring by a complexing agent. This competitive binding activation should shift the equilibrium of the complexation−decomplexation process involving the supermolecule[9] at the pore openings by trapping the dissociated DB24C8 rings and preventing them from recomplexing with

* Authors to whom correspondence should be addressed. J. F. Stoddart: Tel., 310-206-7078; fax, 310-206-1843; e-mail, stoddart@chem.ucla.edu. J. I. Zink: Tel., 310-825-1001; fax, 310-206-4038; e-mail, zink@chem.ucla.edu.

[†] Present address: Center of Novel Functional Molecules, Department of Chemistry, The Chinese University of Hong Kong, Hong Kong, People's Republic of China.

[‡] Present address: Advanced Technology and Systems Analysis Division, Center for Naval Analyses, 4825 Mark Center Drive, Alexandria, VA 22311.

(1) (a) Kresge, C. T.; Leonowicz, M. E.; Roth, W. J.; Vartuli, J. C.; Beck, J. S. *Nature* **1992**, *359*, 710−712. (b) Lu, Y.; Ganguli, R.; Drewien, C. A.; Anderson, M. T.; Brinker, C. J.; Gong, W.; Guo, Y.; Soyez, H.; Dunn, B.; Huang, M. H.; Zink, J. I. *Nature* **1997**, *389*, 364−368.

(2) (a) Zhao, D.; Yang, P.; Melosh, N.; Feng, J.; Chmelka, B. F.; Stucky, G. *Adv. Mater.* **1998**, *10*, 1380−1385. (b) Hernandez, R.; Franville, A.-C.; Minoofar, P. N.; Dunn, B. S.; Zink, J. I. *J. Am. Chem. Soc.* **2001**, *123*, 1248−1249. (c) Minoofar, P. N.; Hernandez, R.; Chia, S.; Dunn, B. S.; Zink, J. I.; Franville, A.-C. *J. Am. Chem. Soc.* **2002**, *124*, 14388−14396.

(3) Liu, N.; Dunphy, D. R.; Atanassov, P.; Bunge, S. D.; Chen, Z.; López, G. P.; Boyle, T. J.; Brinker, C. J. *Nano Lett.* **2004**, *4*, 551−554.

(4) Lai, C.-Y.; Trewyn, B. G.; Jeftinija, D. M.; Jeftinija, K.; Xu, S.; Jeftinija, S.; Lin, V. S.-Y. *J. Am. Chem. Soc.* **2003**, *125*, 4451−4459.

(5) (a) Hernandez, R.; Tseng, H.-R.; Wong, J. W.; Stoddart, J. F.; Zink, J. I. *J. Am. Chem. Soc.* **2004**, *126*, 3370−3371. (b) Nguyen, T. D.; Tseng, H.-R.; Celestre, P. C.; Flood, A. H.; Liu, Y.; Stoddart, J. F.; Zink, J. I. *Proc. Natl. Acad. Sci. U.S.A.* **2005**, *102*, 10029−10034.

(6) Mal, N. K.; Fujiwara, M.; Tanaka, Y. *Nature* **2003**, *421*, 350−353.

(7) (a) Kwon, I. C.; Bae, Y. H.; Kim, S. W. *Nature* **1991**, *354*, 291−293. (b) Fu, Q.; Rama Rao, G. V.; Ista, L. K.; Wu, Y.; Andrzejewski, B. P.; Sklar, L. A.; Ward, T. L.; López, G. P. *Adv. Mater.* **2003**, *15*, 1262−1266. (c) Rudzinski, W. E.; Chipuk, T.; Dave, A. M.; Kumbar, S. G.; Aminabhavi, T. M. *J. Appl. Polym. Sci.* **2003**, *87*, 394−403.

(8) Nguyen, T. D.; Leung, K. C.-F.; Liong, M.; Pentecost, C. D.; Stoddart, J. F.; Zink, J. I. *Org. Lett.* **2006**, *8*, 3363−3366.

10.1021/cm061682d CCC: $33.50 
Published on Web 11/08/2006

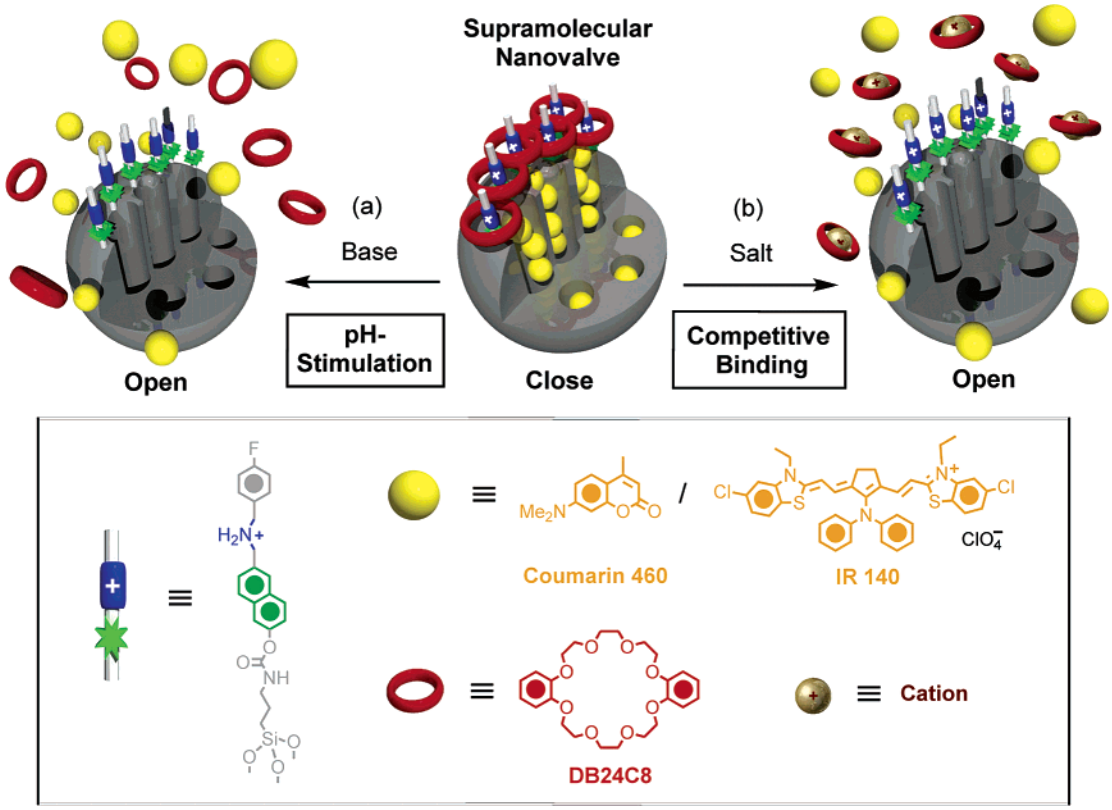


**Figure 1.** Graphical representations of operating supramolecular nanovalves from DB24C8/dialkylammonium tethered porous silica particles MCM-41 (with cross section). The nanovalves can be opened by either (a) pH stimulation with bases or (b) competitive binding with metal/fluorodialkylammonium cations, to trigger controlled release of the luminescent probe molecules, coumarin 460 or IR 140.

the stalks. In this paper, we compare the competitive binding activation of the valve with activation by competitive binding. By the systematic choice of stimuli, we can identify and force the nanovalves' mechanism of operation to follow two possible pathways as shown in Figure 1, namely, either (a) proton abstraction or (b) competitive binding.

## Experimental Section

**Materials.** 4-Fluorobenzylamine (**4**) is commercially available while compound **1**[10] was synthesized according to a literature procedure. The fluorodialkylammonium salts **$F_2$-DBA·$PF_6$**, **$F_4$-DBA·$PF_6$**, and **$(CF_3)_4$-DBA·$PF_6$** were synthesized according to literature procedures.[11] Distilled and deionized $H_2O$ was obtained from Millipore. Other analytical and reagent grade chemicals were purchased from the following suppliers and used without further purification unless specified: tetraethoxysilane (TEOS, 98%, Aldrich), cetyltrimethylammonium bromide (CTAB, 99%, Aldrich), isocyanatopropyltriethoxysilane (ICPES, 95%, Aldrich, redistilled prior to use), pyridinium chlorochromate (PCC, 98%, Aldrich), $NaBH_4$ (99%, Aldrich), $LiAlH_4$ (95%, Aldrich), di-*tert*-butyldicarbonate ($Boc_2O$, 99%, Aldrich), Pd−C (10% Pd, Aldrich), 4-dimethylaminopyridine (99%, Aldrich), $NH_4OH$ solution (28−30%, EMD), $CH_2Cl_2$ (anhydrous, 99.8%, Aldrich), EtOH (200 proof, Pharmaco-AAPER), MeOH (anhydrous, 99.8%, EMD), PhMe (99.5%, EMD), tetrahydrofuran (THF, anhydrous, 99.9%, Aldrich), trifluoroacetic acid (TFA, 99.5%, Merck), triethylamine (TEA, 99%, Acros), *N*,*N*′-diisopropylethylamine (DIPEA, redistilled, 99.5%, Aldrich), hexamethylphosphorous triamide (HMPT, 97%, Acros), $LiOH·H_2O$ (98%, Aldrich), LiCl (99%, Aldrich), KCl (99%, Fisher), $CaCl_2$ (anhydrous, 99.9%, Aldrich), CsCl (anhydrous, 99.9%, Aldrich), CsI (99.9%, Aldrich), coumarin 460 (Exciton), IR 140 (Exciton). All the new compounds that have been synthesized have purities in excess of 98%.

**General Methods.** All reactions were performed under an argon atmosphere unless otherwise stated. Thin layer chromatography (TLC) was performed on silica gel 60 $F_{254}$ (Merck). Column chromatography was performed on silica gel 60F (Merck 9385, 0.040−0.063 mm). All nuclear magnetic resonance (NMR) spectra were recorded on a Bruker Avance 500 ($^1$H: 500 MHz; $^{13}$C: 126 MHz) spectrometer and $CDCl_3$ was used as the solvent. Chemical shifts are reported as parts per million (ppm) downfield from the $Me_4Si$ resonance as the internal standard for both $^1$H and $^{13}$C NMR spectroscopies. Electrospray ionization (ESI) mass spectra were measured on a VG ProSpec triple focusing mass spectrometer with MeCN as the mobile phase. High-resolution ESI (HR-ESI) and matrix-assisted laser-desorption ionization (HR-MALDI) spectra were measured on an IonSpec Fourier transform mass spectrometer. The reported molecular mass (*m*/*z*) values correspond to the most

(9) (a) Ashton, P. R.; Campbell, P. J.; Chrystal, E. J. T.; Glink, P. T.; Menzer, S.; Philp, D.; Spencer, N.; Stoddart, J. F.; Tasker, P. A.; Williams, D. J. *Angew. Chem., Int. Ed. Engl.* **1995**, *34*, 1865−1869. (b) Ashton, P. R.; Chrystal, E. J. T.; Glink, P. T.; Menzer, S.; Schiavo, C.; Spencer, N.; Stoddart, J. F.; Tasker, P. A.; White, A. J. P.; Williams, D. J. *Chem. Eur. J.* **1996**, *2*, 709−728. (c) Ashton, P. R.; Glink, P. T.; Stoddart, J. F.; Tasker, P. A.; White, A. J. P.; Williams, D. J. *Chem. Eur. J.* **1996**, *2*, 729−736. (d) Ashton, P. R.; Ballardini, R.; Balzani, V.; Gómez-López, M.; Lawrence, S. E.; Martínez-Díaz, M.-V.; Montalti, M.; Piersanti, A.; Prodi, L.; Stoddart, J. F.; Williams, D. J. *J. Am. Chem. Soc.* **1997**, *119*, 10641−10651.

(10) Jullien, L.; Canceill, J.; Valeur, B.; Bardez, E.; Lefevre, J.-P.; Lehn, J.-M.; Marchi-Artzner, V.; Pansu, R. *J. Am. Chem. Soc.* **1996**, *118*, 5432−5442.

(11) (a) Cantrill, S. J.; Youn, G. J.; Stoddart, J. F. *J. Org. Chem.* **2001**, *66*, 6857−6872. (b) Fulton, D. A.; Cantrill, S. J.; Stoddart, J. F. *J. Org. Chem.* **2002**, *67*, 7968−7981. (c) Horn, M.; Ihringer, J.; Glink, P. T.; Stoddart. J. F. *Chem. Eur. J.* **2003**, *9*, 4046−4054. (d) Lowe, J. N.; Fulton, D. A.; Chiu, S.-H.; Elizarov, A. M.; Cantrill, S. J.; Rowan, S. J.; Stoddart, J. F. *J. Org. Chem.* **2004**, *69*, 4390−4402.

abundant monoisotopic masses. X-ray diffraction (XRD) analysis was performed using Philips X'Pert Pro. Scanning electron microscopic (SEM) image was collected using a JEOL SM-71010 apparatus. Gold coating of the material for SEM imaging was performed with a Gold Sputterer (Hummer 6.2, Anatech Ltd., plasma discharge current = 15 mA at 70 mTorr, 2 min). Nitrogen isotherms were measured using Micromeritics ASAP 2000. The controlled release of coumarin 460 into solution was monitored over time using luminescence spectroscopy (Acton SpectraPro 2300i CCD).

**Alcohol 2.** A mixture of the ester **1**[10] (1.6 g, 5.5 mmol) in THF (10 mL) was added dropwise to a slurry of $LiAlH_4$ (420 mg, 11 mmol) in THF (10 mL) at 0 °C. The reaction mixture was allowed to stir for 3 h at 25 °C under Ar (1 atm). Subsequently, the mixture was quenched carefully by the dropwise addition of $H_2O$ (1 mL) and then 1 M HCl (30 mL), followed by two consecutive extractions with EtOAc (20 mL). The combined organic extracts were dried ($MgSO_4$) and filtered. The filtrate was concentrated under reduced pressure and the residue was purified by column chromatography using hexanes/EtOAc (2:1) as the eluent to give the alcohol **2** (1.4 g, 97% yield) as a white solid. mp: 120.6−123.8 °C. $^1$H NMR: $\delta$ 1.70 (t, $J$ = 5 Hz, 1 H), 4.83 (d, $J$ = 5 Hz, 2 H), 5.19 (s, 2 H), 7.21−7.25 (m, 2 H), 7.32−7.50 (m, 6 H), 7.70−7.76 (m, 3 H). $^{13}$C NMR: $\delta$ 65.5, 69.9, 106.9, 119.2, 125.5, 127.1, 127.2, 128.0, 128.4, 128.6, 129.3, 129.4, 133.9, 136.0, 136.7, 156.8. MS(HR-ESI): calcd for $C_{18}H_{16}O_2$ $m/z$ = 264.1150; found $m/z$ = 264.1138 [$M^+$, 100%].

**Aldehyde 3.** A mixture of the alcohol **2** (200 mg, 0.76 mmol) and pyridinium chlorochromate (PCC) (330 mg, 1.5 mmol) in $CH_2Cl_2$ (5 mL) was stirred at 25 °C under Ar (1 atm) for 2 h prior to filtration through a short pad of silica gel. The filtrate was then concentrated under reduced pressure. The residue was purified by column chromatography using hexanes/EtOAc (5:1) as the eluent to afford the aldehyde **3** (0.19 g, 98% yield) as a white solid. mp: 126.4−129.2 °C. $^1$H NMR: $\delta$ 5.17 (s, 2 H), 7.00 (d, $J$ = 9.2 Hz, 1 H), 7.28−7.38 (m, 6 H), 7.55 (d, $J$ = 8.4 Hz, 1 H), 7.69−7.76 (m, 2 H), 7.92 (d, $J$ = 9.2 Hz, 1 H), 9.98 (s, 1 H). $^{13}$C NMR: $\delta$ 70.0, 107.0, 119.5, 125.6, 127.2, 127.3, 128.1, 128.4, 128.7, 129.4, 134.0, 136.3, 140.0, 160.0, 190.1. MS(HR-ESI): calcd for $C_{18}H_{14}O_2$ $m/z$ = 262.0994; found $m/z$ = 262.1003 [$M^+$, 100%].

**Amine 5.** A mixture of the 4-fluorobenzylamine **4** (0.70 mL, 5.3 mmol) and the aldehyde **3** (1.4 g, 5.3 mmol) in PhMe (20 mL) was stirred and heated under reflux in a Dean−Stark apparatus for 12 h. Subsequently, the mixture was cooled to room temperature and excess of solvent was evaporated off under reduced pressure to afford an oil. Next, the resulting oil was redissolved in a THF/MeOH (2:1, 30 mL) mixture and $NaBH_4$ (0.61 g, 16 mmol) was added portionwise at 0 °C. The reaction mixture was then stirred at 25 °C for 12 h. $H_2O$ (30 mL) was added dropwise to quench the reaction and the resulting mixture was extracted with EtOAc (2 × 20 mL). The combined organic extracts were dried ($MgSO_4$) and filtered. The filtrate was concentrated under reduced pressure and the residue was purified by column chromatography using hexanes/EtOAc (3:1) as the eluent to give the amine **5** (1.8 g, 91% yield) as a white solid. mp: 67.6−69.8 °C. $^1$H NMR: $\delta$ 1.74 (brs, 1 H), 3.81 (s, 2 H), 3.93 (s, 2 H), 5.18 (s, 2 H), 7.00−7.05 (m, 3 H), 7.28−7.45 (m, 7 H), 7.50 (d, $J$ = 7.4 Hz, 2 H), 7.67−7.75 (m, 3 H). $^{13}$C NMR: $\delta$ 49.1, 52.2, 69.9, 107.1, 114.9, 115.1, 119.1, 119.2, 126.3, 127.0, 128.4, 128.9, 129.0, 129.1, 129.2, 129.5, 133.6, 135.2, 136.8, 156.6, 162.9. MS(HR-ESI): calcd for $C_{25}H_{22}FNO$ $m/z$ = 371.1685; found $m/z$ = 371.1690 [$M^+$, 100%].

***N*-Boc-Protected Amine 6.** $Boc_2O$ (1.3 g, 5.8 mmol) in THF (10 mL) was added dropwise to a mixture of the amine **5** (1.8 g, 4.9 mmol), $Et_3N$ (1.4 mL, 9.7 mmol), and a catalytic amount of *N*,*N*′-dimethylaminopyridine in THF (15 mL) at 0 °C under Ar (1 atm). The reaction mixture was stirred at 25 °C for 12 h before it was quenched by the addition of $H_2O$ (20 mL). Subsequently, the resulting mixture was extracted with EtOAc (2 × 20 mL). The combined organic extracts were dried ($MgSO_4$) and filtered and the filtrate was concentrated under reduced pressure to give a residue, which was purified by column chromatography using hexanes/EtOAc (6:1) as the eluent to afford the *N*-Boc-protected amine **6** (2.3 g, 98% yield) as a white solid. mp: 79.4−81.6 °C. $^1$H NMR: $\delta$ 1.56 (s, 9 H), 4.22−4.50 (br, 4 H), 5.19 (s, 2 H), 7.01 (dd, $J$ = 8.6 Hz, 4 H), 7.15−7.25 (br, 3 H), 7.36 (d, $J$ = 7.2 Hz, 2 H), 7.38−7.43 (m, 2 H), 7.50 (d, $J$ = 7.2 Hz, 2 H), 7.68−7.75 (m, 2 H). $^{13}$C NMR: $\delta$ 28.6, 48.4, 49.3, 60.3, 76.7, 107.0, 115.2, 119.2, 126.6, 127.2, 127.5, 127.9, 128.5, 128.8, 128.9, 129.1, 129.5, 132.9, 133.7, 136.7, 156.7, 161.0, 162.9. MS(HR-ESI): calcd for $C_{30}H_{30}FNNa$ $m/z$ = 494.2102; found $m/z$ = 494.2104 [$(M + Na)^+$, 100%].

**Naphthol 7.** A mixture of the *N*-Boc-protected amine **6** (1.4 g, 3.0 mmol) and palladium on carbon (10% Pd, 0.10 g) in EtOH/EtOAc (1:1, 20 mL) was stirred under $H_2$ (balloon pressure) at 25 °C for 6 h. Subsequently, the mixture was filtered through a short pad of Celite and the filtrate was then concentrated under reduced pressure. The residue was purified by column chromatography using hexanes/EtOAc (3:1) as the eluent to afford the alcohol **7** (0.80 g, 71% yield) as a white solid. mp: 106.0−108.2 °C. $^1$H NMR: $\delta$ 1.52 (s, 9 H), 4.20−4.55 (br, 4 H), 5.97 (brs, 1 H), 6.96−7.05 (m, 4 H), 7.14−7.25 (br, 4 H), 7.60 (d, $J$ = 8.6 Hz, 1 H), 7.66 (d, $J$ = 8.6 Hz, 1 H). $^{13}$C NMR: $\delta$ 28.3, 48.6, 49.3, 85.1, 109.3, 115.3, 118.2, 125.9, 126.5, 128.3, 129.0, 129.3, 129.5, 133.9, 153.9, 155.8, 161.0, 162.9. MS(HR-ESI): calcd for $C_{23}H_{24}FNO_3Na$ $m/z$ = 404.1632; found $mz$ = 404.1642 [$(M + Na)^+$, 100%].

**General Preparation of the Porous Silica Particle MCM-41-Based Nanovalves.** MCM-41 was prepared according to a literature procedure.[12a−g] Surfactants were removed by either calcination at 550 °C for 5 h or solvent extraction (2.0 g of the material was heated under reflux in methanolic HCl (220 mL of MeOH and 2.5 mL of concentrated HCl)). Successful surfactant removal was confirmed by the shifts in Bragg peaks and also by the large increase in volume of $N_2$ adsorbed as indicated by $N_2$ isotherm. Attachment or incorporation of molecules in silica prepared by the sol−gel method[12a−g] has been studied.

The surfactant-removed MCM-41 was derivatized first of all with isocyanatopropyltriethoxysilane (ICPES) using a gas-phase reaction. The powder was then placed on a filter frit above the solution, followed by refluxing with the ICPES linker in PhMe for 12 h under $N_2$ (1 atm). The ICPES-derivatized material was soaked in PhMe for 1 d to remove surface-adsorbed ICPES, followed by filtering and drying under reduced pressure. Refluxing ICPES-modified MCM-41 in a $CH_2Cl_2$ solution of the naphthyl dialkylammonium precursor (**7**) for 1 d under $N_2$ (1 atm) afforded the dialkylammonium-tethered MCM-41. The surface silanol coverage of silica particles prepared in a manner similar to ours has been reported to be about 2.4 silanols/nm$^2$.[12h] There are about 7.8 silicon atoms/nm;[2,12i] thus, roughly one-third of all silicon atoms are in

(12) (a) Miller, J. M.; Dunn, B. S.; Valentine, J. S.; Zink, J. I. *J. Non-Cryst. Solids* **1996**, *202*, 279−289. (b) Dave, B. C.; Miller, J. M.; Dunn, B. S.; Valentine, J. S.; Zink, J. I. *J. Sol-Gel Sci. Technol.* **1997**, *8*, 629−634. (c) Grün, M.; Laner, I.; Unger, K. K. *Adv. Mater.* **1997**, *9*, 254−257. (d) Dunn, B. S.; Miller, J. M.; Dave, B. C.; Valentine, J. S.; Zink, J. I. *Acta Mater.* **1998**, *46*, 737−741. (e) Huang, M. H.; Dunn, B. S.; Soyez, H.; Zink, J. I. *Langmuir* **1998**, *14*, 7331−7333. (f) Chia, S.; Jun, U.; Tamanoi, F.; Dunn, B. S.; Zink, J. I. *J. Am. Chem. Soc.* **2000**, *122*, 6488−6489. (g) Minoofar, P. N.; Dunn, B. S.; Zink, J. I. *J. Am. Chem. Soc.* **2005**, *127*, 2656−2665. (h) Zhao, X. S.; Lu, G. Q.; Whittaker, A. K.; Millar, G. J.; Zhu, H. Y. *J. Phys. Chem. B* **1997**, *101*, 6525−6531. (i) Iler, R. K. *The Chemistry of Silica*; Wiley: New York, 1979.

the form of silanol. Derivatization using excess ICPES is almost quantitative. Based on these data, there are on average approximately two to three pseudorotaxanes around the circumference of a 2 nm diameter pore. The addition of 3 equiv of TFA to the material in $CH_2Cl_2$ solution for 2 h yielded the corresponding dialkylammonium salt with $CF_3CO_2^-$ counterion. The loading of guest molecules was achieved by soaking the derivatized material in a solution of coumarin 460 or IR 140 at a concentration of 0.4 mM. The loaded material was capped with 1 equiv of DB24C8 in $CH_2Cl_2$. The material was washed extensively with $CH_2Cl_2$ to remove surface-adsorbed probe molecules.

## Results and Discussion

**Synthesis and Characterization.** The naphthyl precursor **7** was synthesized as outlined in Scheme 1. First, the methyl ester **1**[10] (Bn = benzyl) was reduced by $LiAlH_4$ in tetrahydrofuran (THF) to afford the alcohol **2** in 97% yield. Subsequently, the alcohol **2** was oxidized to the corresponding aldehyde **3** in 98% yield with pyridinium chlorochromate (PCC). Then, the aldehyde **3** and 4-fluorobenzylamine (**4**) were dissolved in PhMe and heated under reflux in a flask equipped with a Dean−Stark apparatus to remove the $H_2O$ formed from the reaction, which in turn on addition of $NaBH_4$ gave the corresponding amine **5** in 91% yield. The free amine **5** was treated with $Boc_2O$ (Boc = *tert*-butyloxycarbonyl), resulting in the formation of the *N*-Boc-protected amine **6** in 98% yield. Finally, compound **6** was debenzylated, using Pd-catalyzed hydrogenolysis conditions, to give the naphthol **7** in 71% yield. The hydroxyl group present in compound **7** is essential (vide infra) for the attachment to the isocyanatopropyltriethoxysilane (ICPES)-tethered mesoporous silica particles.

**Scheme 1. Synthesis of Naphthyl Compound 7**

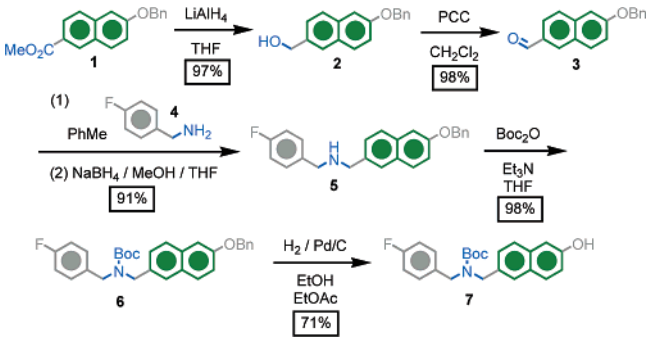


Mesoporous silica, namely, MCM-41, was used as (a) the supporting platform for the movable elements and (b) the nanocontainers of the probe molecules. Using a modification of Stober's synthesis of monodisperse silica, for which aqueous ammonia was used as a morphology catalyst, nanostructured silica was obtained that consists of near-spherical silica particles with an average diameter of 600 nm, as verified by scanning electron microscopy (see Supporting Information).[12a−g] With use of cetyltrimethylammonium bromide as the template, the highly ordered pores form a two-dimensional hexagonal structure that has a lattice spacing of 3.6 nm as measured by X-ray diffraction. The surfactant was removed by calcination for 5 h at 550 °C. $N_2$ adsorption/desorption isotherms at 77 K were used to investigate the porosity of the material, which exhibits a high surface area (929.7 $m^2/g$). When the Barret−Joyner−Halenda (BJH) method of calculation was employed, the inner diameters of the pores were calculated to be 2 nm.[12a−g] $N_2$ adsorption/desorption isotherms also revealed that the pores are empty after calcinations and, as such, they are accessible and suitable for use as molecular containers. The porous silica was derivatized (Scheme 2) with ICPES to afford the isocyanate-terminated porous silica, which was then linked to the hydroxyl group of the dialkylammonium precursor **7**. The material was treated with TFA to afford the dialkylammonium ion-tethered mesoporous silica. Controlled release experiments of phenyl and anthracenyl nanovalves, which have molecular structures similar to the naphthyl nanovalves, have been performed (see Supporting Information) as model investigations. The results obtained with these nanovalves can be regarded as controls when evaluating the performance of the naphthyl nanovalves.

Mechanically interlocked molecules possessing switchable capabilities have been explored[13] as prototypes for electronics components, nanoscale muscles, and nanovalves. The myriad of methods of chemical derivatization and modification that have been conferred upon this class of molecules allows them to be integrated into a variety of materials and to be controllable by a range of external stimuli.[14] A host−guest [2]pseudorotaxane system, which consists of the DB24C8 host and the secondary dialkylammonium ion guest, actuated by Bronstead bases, was demonstrated recently.[15,16] In the context of nanovalve construction, the binding of host−guest species involving the rings (DB24C8) and stalks (dialkylammonium ion tethered at the nanopore orifices) constitutes the closed configuration. Upon the dissociation of this host−guest species, the nanovalves are opened.

The release of probe molecules from the hybrid MCM-41 into the supernatant was measured by monitoring the emission spectrum in the solution above the MCM-41

(13) (a) Balzani, V; Credi, A.; Raymo, F. M.; Stoddart, J. F. *Angew. Chem., Int. Ed.* **2000**, *39*, 3348−3391. (b) Balzani, V.; Credi, A.; Venturi, M. *Molecular Devices and Machines − A Journey into the Nano World*; Wiley−VCH: Weinheim, 2003. (c) Liu, Y; Flood, A. H.; Bonvallet, P. A.; Vignon, S. A.; Northrop, B. N.; Tseng, H.-R.; Jeppesen, J.; Huang, T. J.; Brough, B.; Baller, M.; Magonov, S.; Solares, S.; Goddard, W. A., III; Ho, C.-M.; Stoddart, J. F. *J. Am. Chem. Soc.* **2005**, *127*, 9745−9759. (d) Balzani, V.; Credi, A.; Ferrer, B.; Silvi, S.; Venturi, M. *Top. Curr. Chem.* **2005**, *262*, 1−27. (e) Moonen, N. N. P.; Flood, A. H.; Fernández, J. M.; Stoddart, J. F. *Top. Curr. Chem.* **2005**, *262*, 99−132. (f) Kay, E. R.; Leigh, D. A. *Top. Curr. Chem.* **2005**, *262*, 133−177. (g) Braunschweig, A. B.; Northrop, B. H.; Stoddart, J. F. *J. Mater. Chem.* **2006**, *16*, 32−44.

(14) (a) Glink, P. T.; Schiavo, C.; Stoddart, J. F.; Williams, D. J. *Chem. Commun.* **1996**, 1483−1490. (b) Hubin, T. J.; Kolchinski, A. G.; Vance, A. L.; Busch, D. H. *Adv. Supramol. Chem.* **1999**, *5*, 237−357. (c) Hubin, T. J.; Busch, D. H. *Coord. Chem. Rev.* **2000**, *200−202*, 5−52. (d) Cantrill, S. J.; Pease, A. R.; Stoddart, J. F. *J. Chem. Soc., Dalton Trans.* **2000**, 3715−3734. (e) Aricó, F.; Badjić, J. D.; Cantrill, S. J.; Flood, A. H.; Leung, K. C.-F.; Liu, Y.; Stoddart, J. F. *Top. Curr. Chem.* **2005**, *249*, 203−259.

(15) (a) Ashton, P. R.; Ballardini, R.; Balzani, V.; Baxter, I.; Credi, A.; Fyfe, M. C. T.; Gandolfi, M. T.; Gómez-López, M.; Martínez-Díaz, M.-V.; Piersanti, A.; Spencer, N.; Stoddart, J. F.; Venturi, M.; White, A. J. P.; Williams, D. J. *J. Am. Chem. Soc.* **1998**, *120*, 11932−11942. (b) Elizarov, A. M; Chiu, S.-H.; Stoddart, J. F. *J. Org. Chem.* **2002**, *67*, 9175−9181. (c) Badjić, J. D.; Balzani, V.; Credi, A.; Silvi, S.; Stoddart, J. F. *Science* **2004**, *303*, 1845−1849. (d) Badjić, J. D.; Ronconi, C. M.; Stoddart, J. F.; Silvi, S.; Credi, A.; Balzani, V. *J. Am. Chem. Soc.* **2006**, *128*, 1489−1499.

(16) Shukla, R.; Kida, T.; Smith, B. D. *Org. Lett.* **2000**, *2*, 3099−3102.

**Scheme 2. Synthesis of the Naphthyl Nanovalves**

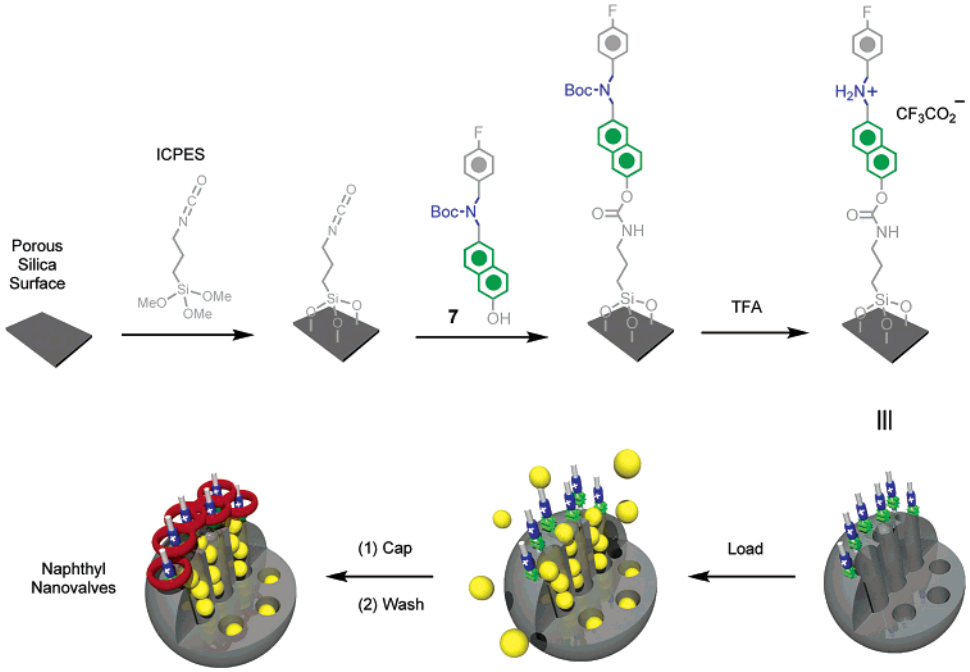


powder. The functional material was placed in a cell holder, such that only the $CH_2Cl_2$ liquid above the powder solution is exposed to excitation light. The luminescence of released probe molecules in solution was monitored over time. The solution was stirred at a low stirring rate to create a homogeneous solution at any given time. Stimuli were added at a designated time to trigger the controlled release. For the purpose of comparison between the rates of release using different stimuli, the concentration and volume of stimuli were kept constant. In all cases, the experiments were performed in 10 mL of $CH_2Cl_2$ containing 20 mg of silica particles. In the case of using bases as stimuli, the liquid bases (30 $\mu$L) were added directly into the spectroscopic cell at a designated time. In the case of using fluorodialkylammonium salts as the stimuli, they were dissolved in $CH_2Cl_2$ (19 mM) and 30 $\mu$L of the salt solution was added at a designated time. When different alkali metal and alkaline earth metal salts were used, the salts were dissolved in EtOH or MeOH (19 mM) and 30 $\mu$L of the salt solution was added at a designated time.

In the first section, we demonstrate opening of the nanovalves by proton abstraction. In the second section, we demonstrate that the conjugate acids of the dialkylammonium stalks stimulate opening of the nanovalves by competitive binding. Finally, we demonstrate activation by alkali and alkaline earth metal ions.

**1. Activation by Deprotonation.** The functioning of the nanovalves depends on whether the moving parts can block the trapped molecules from leaking out when the nanovalves are closed and on the efficiency of their movement away from the pores to release the trapped molecules. A range of bases with different basicities and structural properties, including hexamethylphosphorous triamide (HMPT), *N*,*N*′-diisopropylethylamine (DIPEA), and triethylamine (TEA), was employed to effect the controlled release of coumarin 460. The slight increase in the emission intensity indicates (Figure 2) a small amount of leakage from the closed nanovalves. The release of coumarin 460 from the pores upon activation by addition of HMPT (Figure 2a) was characterized by a lag time of 200 s. After this delay, the guest molecules were released at a much faster rate, as indicated by a much steeper slope. The half-life ($t_{1/2}$) is defined as the time the system takes to release half of the content. For HMPT-triggered release, $t_{1/2}$ is 450 ± 30 s. The $t_{1/2}$ for DIPEA-activated release (Figure 2b) is 300 ± 30 s. With TEA as the base, no lag time is observed (Figure 2c) and the $t_{1/2}$ decreases further to 100 ± 20 s. All three samples were left standing overnight and the resulting emission intensities were used to define the total amounts released.

Since all the experimental conditions used to trigger the release of the guest molecules were the same, a direct comparison between the different release profiles, based on the nature of the triggering bases, can be made. Comparing the three bases, the controlled release—according to the

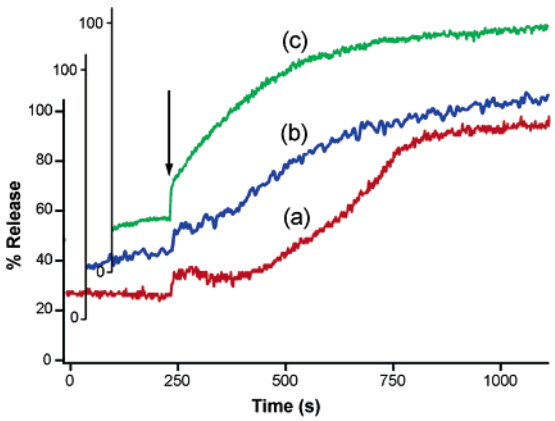


**Figure 2.** Controlled release of coumarin 460 from the dialkylammonium/DB24C8-MCM-41 nanovalves in $CH_2Cl_2$ triggered by (a) hexamethylphosphorous triamide, (b) *N*,*N*′-diisopropylethylamine, and (c) triethylamine, as monitored by luminescence spectroscopy over time. The arrow indicates the triggering time. 100% Release represents the total amount of release 24 h after the triggering time.

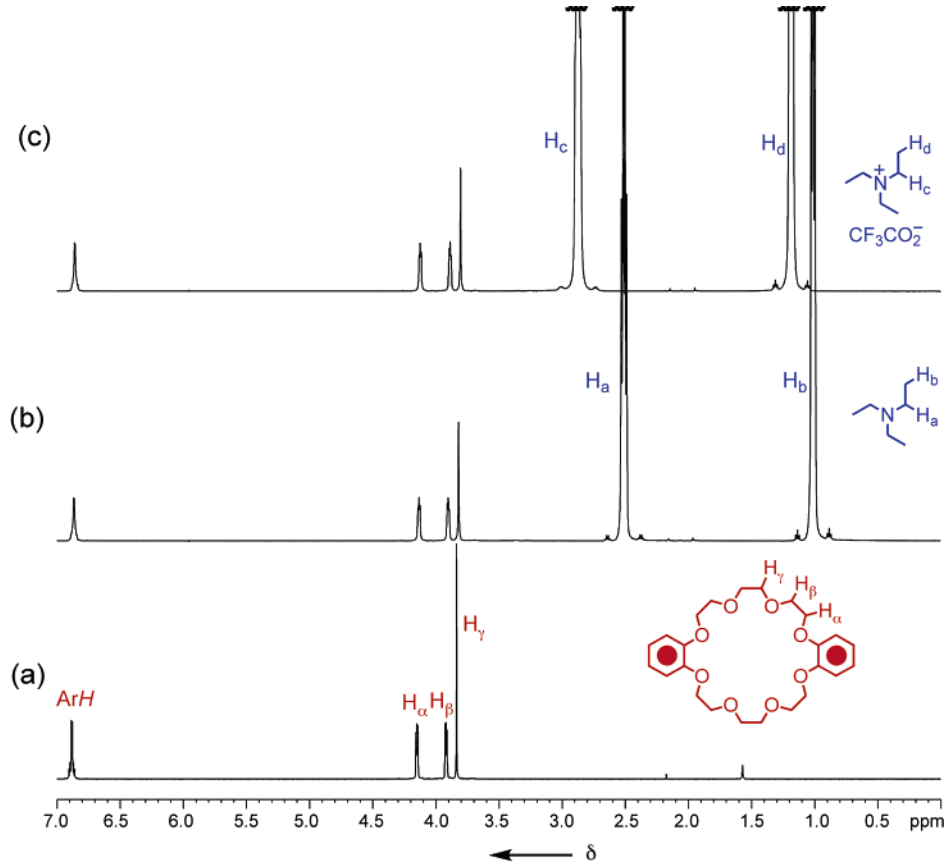


**Figure 3.** $^1$H NMR spectra ($CDCl_3$, 298 K, 500 MHz) of the DB24C8 binding experiments. (a) DB24C8, (b) DB24C8 after the addition of TEA, and (c) DB24C8 after the addition of TEA and then TFA. These results indicate that DB24C8 has no interaction with TEA and the salt $Et_3NH^+ \cdot CF_3CO_2^-$.

deprotonation mechanism—is governed by the basicity and the steric hindrance of the bases employed. DIPEA and TEA have similar basicities, as reflected by their $pK_a$ values being 9.0 and 8.5, respectively, in $Me_2SO$. The rate of release using DIPEA is lower than that when using TEA. This result indicates that the more bulky DIPEA—despite being the stronger base—deprotonates the complex tethered to the silica particles more slowly, thus affecting the rate of operation of the nanovalves. When an even more bulky and weaker base (HMPT) is used, the rate of release is even slower. HMPT- and DIPEA-activated releases exhibit lag times, whereas release activated by TEA does not. The lag time observed for HMPT is longer than that for DIPEA, signifying a stronger impact on the part of steric hindrance. As a result, the variation of the bases having different steric properties and basicities manifests itself in the three different release rates such that TEA > DIPEA > HMPT.

The selection of the bases for the activation of the nanovalves also serves another purpose—that is, to differentiate between the protonation/deprotonation and competitive binding mechanisms. The equilibrium (complexation−decomplexation) processes of the rings and the stalks are slow enough to be observed on the $^1$H NMR time scale. If the added base can bind to the short-lived dissociated DB24C8, then the base could affect the operation of the nanovalves by means of the competitive binding mechanism in concert with the proton abstraction mechanism. This is not the case since HMPT, a large base, is too large to fit into the cavity of DB24C8 ring and trigger the nanovalves as the result of a competitive binding mechanism.[17] Yet HMPT can trigger the controlled release. This observation implies that the bases trigger the nanovalves by the deprotonation mechanism.

To verify that the operation of the nanovalves using bases occurs by the deprotonation mechanism instead of a competitive binding one, a binding experiment between DB24C8 and a chosen base was performed in solution and characterized (Figure 3) by $^1$H NMR spectroscopy. On mixing DB24C8 with an excess of TEA (30 equiv) in $CDCl_3$ at 25 °C, no change in the chemical shifts of proton resonances of the DB24C8 ($H_\alpha$, $H_\beta$, and $H_\gamma$) are observed. This observation indicates that there is no interaction between DB24C8 and TEA. Subsequently, an excess of TFA was added to the mixture to neutralize and consume all the free bases by forming the corresponding $Et_3NH^+ \cdot CF_3CO_2^-$ salt. The same resonances (for $H_\alpha$, $H_\beta$, and $H_\gamma$) are found for the DB24C8/salt mixture and for free DB24C8, confirming that the salt also does not interact with the crown ether. Similar experiments were performed using DIPEA and HMPT, revealing that they also do not interact with DB24C8. These studies show that TEA/DIPEA/HMPT function as bases that deprotonate the dialkylammonium ion centers, causing disassembly of the pseudorotaxanes and unlocking of the nanovalves.

Ionic compounds can also be trapped and released. IR 140—an organic ammonium perchlorate laser dye—is a

(17) The 1:1 complex of DB24C8/HMPT was calculated according to the molecular mechanics calculation (MM2) using CS Chem 3D Ultra, 8.0 ed.; Cambridge Soft Corporation: Cambridge, 2003.

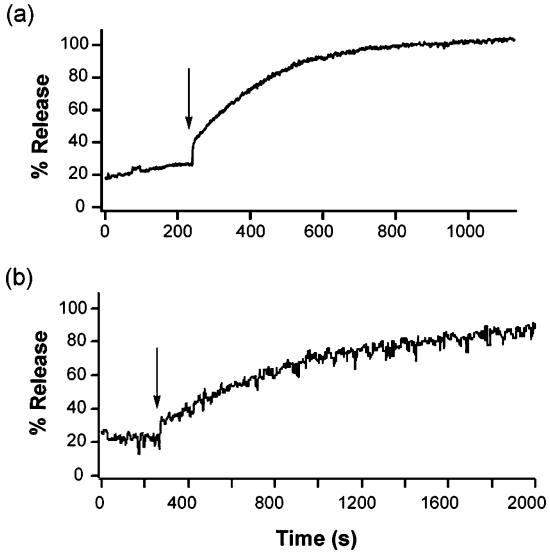


**Figure 4.** Controlled release of (a) coumarin 460 and (b) IR 140, triggered by TEA in the naphthyl DB24C8/dialkylammonium nanovalves in $CH_2Cl_2$ at the time indicated by the arrows.

cationic fluorophore with a larger structure than that of coumarin 460 and it is stable in the presence of bases.[18] IR 140 was loaded into the pores of MCM-41 using the same procedure as described for coumarin 460. The release of IR 140 (Figure 4b) from the naphthyl DB24C8/dialkylammonium nanovalves was monitored using the method described previously. Before the triggered release, the emission baseline of IR 140 rose slowly, suggesting slow leakage. Upon the addition of TEA, the emission intensity of IR 140 in solution showed a rapid increase, followed by a gradual leveling off to a maximum. The similarity between the release profiles of coumarin 460 (Figure 4a) and IR 140 (Figure 4b) using TEA as the stimulus demonstrates that charged molecules do not result in a change in the functioning of the nanovalves. The release rate of IR 140 ($t_{1/2} = 600 \pm 100$), however, is slower than that of coumarin 460, indicating that the charge and/or the larger dimensions of the IR 140 probe molecule plays a role.

**2. Activation by Competitive Binding Using Fluorodialkylammonium Salts.** Activation of the nanovalves by competitive binding of the DB24C8 ring offers the possibility of broadening the range of stimuli. Deprotonation of the dialkylammonium stalks, thus turning off the hydrogen bonding and the electrostatic interactions, is the most obvious method of releasing the rings and opening the nanovalves. Alternatively, providing external binding sites for the DB24C8 rings offer a less obvious but nonetheless effective stimulus for opening the nanovalves. In contrast to direct release by deprotonation, a competitor for the rings could open the nanovalves by shifting the equilibrium. The DB24C8/dialkylammonium nanovalves are dynamic systems in which the rings equilibrate rapidly between the binding sites at the nanopore entrances and the surrounding liquid. The ON rate is much faster than the OFF rate.[19] Operationally, these rates are faster than the rate of escape of the tested probe molecules trapped in the nanopores and so minimal leakage is observed. If cations with a stronger binding affinity than that of the stalks for the DB24C8 rings is added to the system, they will bind to the rings, trapping them in the solution and preventing them from returning to the stalks. The competitive binding mode also operates under equilibrium conditions, but most of the time the DB24C8 rings bind to the competing ions with a stronger binding affinity. If this mechanism could be made operative, it would be expected to decrease the number of closed nanovalves as a function of time, thus allowing the release of the nanopores' contents. We might expect that this type of activation would result in slower release because the rate would depend on the trapping of a small number of unbound DB24C8 rings rather than on the diffusion of a base to the stalks where deprotonation then occurs.

In this section, we discuss the results of an investigation where conjugated acids of organic fluorodialkylammonium salts are the activating agents. The DB24C8 rings bind to these cations more strongly than to the tethered dialkylammonium stalks and so a shift in the equilibrium from closed to open nanovalves is observed.

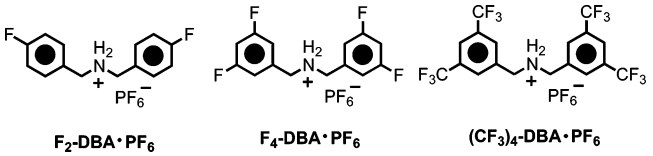


**Figure 5.** Structure formulas of the fluorodialkylammonium salt (**$F_2$-DBA·$PF_6$**, **$F_4$-DBA·$PF_6$**, and **$(CF_3)_4$-DBA·$PF_6$**) used for competitive binding activation of the nanovalves.

Three fluorodialkylammonium salts with an increasing number of F atoms on the dialkylammonium backbone were employed[11] (**$F_2$-DBA·$PF_6$**, **$F_4$-DBA·$PF_6$**, and **$(CF_3)_4$-DBA·$PF_6$**) (Figure 5) to evaluate the effectiveness of the competitive binding mechanism. Since fluorine is a strong electron-withdrawing atom, its presence on the dialkylammonium backbone makes[11] the ammonium recognition site more electron-deficient. Thus, the larger the number of F on a particular ammonium salt, the greater its ability to bind DB24C8 and open the nanovalves. In addition to the electrostatic effects, the competition for the cavities of the dissociated DB24C8 rings using the fluorodialkylammonium salts also involves[11] the size of the organic cation. In this study, fluorodialkylammonium salts of a similar size at identical concentrations were used.

The rate of release of coumarin 460 stimulated (Figure 6) by the three fluorodialkylammonium salts was slow relative to that caused by deprotonation. The rates are similar for all three cations. These results show that activation of the nanovalves by deprotonation—i.e., decreasing the binding constant—is much faster than shifting the equilibrium with similar size organic fluorodialkylammonium salts.

(18) To test for insusceptibility of the probe molecule to the TEA, IR 140 was dissolved in $CH_2Cl_2$ (10 mL of a 0.5 mM solution) and its luminescent spectrum was obtained using a Fluorolog FL3-22 (ISA Spex, Jobin Yvon, Longjumeau, France). Fifty microliters of TEA was added to the IR 140/$CH_2Cl_2$ solution and the luminescence spectrum of the solution was obtained again. No change in luminescence intensity as well as no shift of signals was observed.

(19) (a) Dechter, J. J.; Zink, J. I. *J. Am. Chem. Soc.* **1975**, *97*, 2937−2942. (b) Dechter, J. J.; Zink, J. I. *J. Am. Chem. Soc.* **1976**, *98*, 845−846.

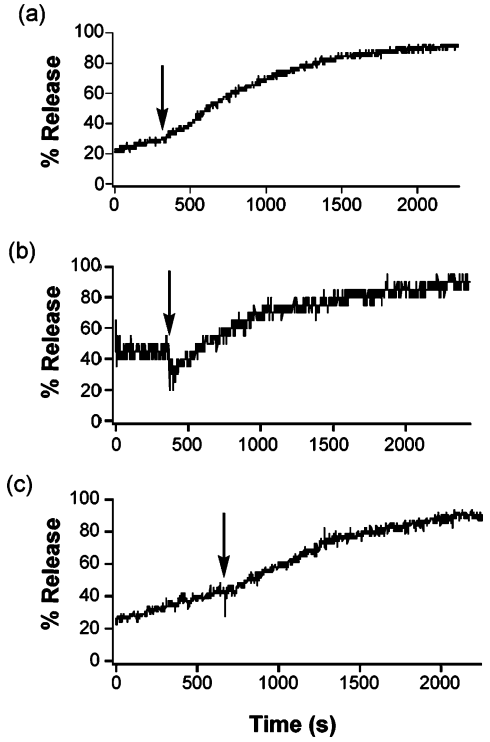


**Figure 6.** Controlled release of coumarin 460 from the naphthyl DB24C8/dialkylammonium nanovalves in $CH_2Cl_2$ caused by (a) **$F_2$-DBA·$PF_6$**, (b) **$F_4$-DBA·$PF_6$**, and (c) **$(CF_3)_4$-DBA·$PF_6$** at the time as indicated by the arrow.

**3. Competitive Binding Activation Using Alkali Metal and Alkaline Earth Metal Salts.** A set of metal mono- and dications selected for their high and low binding affinities to DB24C8 have been used to investigate further the competitive binding mechanism. Crown ethers are best known[20,21] for their ability to bind selectively a large range of metal ions. Central to the concept of selective binding is competitive binding,[11c,22] in which the metal and dialkylammonium cations compete for the crown ether's cavity such that the ion with the largest binding affinity wins. In the context of the operation of nanovalves, the metal cation must compete successfully for the free DB24C8 rings undergoing an equilibrium complexation−decomplexation process. Successful competition by metal cations in close proximities with the dialkylammonium/DB24C8 supramolecular complexes results in the removal of DB24C8 rings from the tethered dialkylammonium stalks. It is of interest to compare the effects of the binding abilities of metal or fluorodialkylammonium salts on the rate of release of the probe molecules.

Four metal ions were selected for their different abilities to complex with DB24C8. The cations range[23] from $Cs^+$ with its high affinity to $Li^+$ with its low affinity for DB24C8. A secondary requirement dictated that the employed metal salt must be compatible with the operation of the nanovalves—i.e., it should not change the luminescence properties of the probe molecules and it must have nonzero solubility in the solvent system used to operate the nanovalves. CsCl, KCl, $CaCl_2$, and LiCl were chosen for investigation. The metal salts were dissolved in EtOH and the same concentrations and amounts of each salt solution were added directly at a designated time to trigger the release.

The rates of release of coumarin 460 from the naphthyl DB24C8/dialkylammonium nanovalves in $CH_2Cl_2$, caused by addition of the salts, are shown in Figure 7. Before salt addition, there is a slight increase in emission intensities, indicating a small amount of leakage. The release of coumarin 460 upon activation by the addition of CsCl/EtOH solution was characterized (Figure 7a) by an immediate large increase in the slope, eventually reaching a plateau at about 800 s. The $t_{1/2}$ is 130 ± 20 s, while the total time for the system takes to release >99% of its contents is 250 ± 50 s. The release caused by $CaCl_2$ was also fast (Figure 7b) with a $t_{1/2}$ of 100 ± 20 s. In contrast to the two fast release rates triggered by $Cs^+$ and $Ca^{2+}$, the releases caused by KCl and LiCl were much slower (Figures 7c and 7d) with $t_{1/2}$ values of 380 ± 50 and 450 ± 50 s, respectively. The control experiment, in which the same volume (30 $\mu$L) of EtOH was added, had no effect upon the release of probe molecules (see Supporting Information) because of the large volume ratio between $CH_2Cl_2$ and EtOH.

The observed rates follow the expected trend: the metal cation with the size most compatible with the DB24C8 cavity causes the fastest operation of the nanovalves. The $Cs^+$ ion has (Table 1) the largest ionic radius,[24] leading to the fastest dethreading rate and the fastest release rate. The addition of $K^+$, a smaller cation, leads to an intermediate release rate and addition of $Li^+$ ion causes the slowest release. The complexation of alkali/alkaline earth metal ions to the crown ethers depends[25] on (a) the cavity size of the crown ether, (b) the ionic radius of the metal cation, (c) the number of donor atoms on the crown ether, (d) the ring conformations in the free and complexed crown ether, and (e) the solvation energy of the metal ion. However, the picture becomes much less clear for crown ethers with very large cavity sizes. For DB24C8, the cavity size effect is no longer dominant since several metal cations ($K^+$, $Rb^+$, and $Cs^+$) can complex well

(20) (a) Lehn, J.-M. *Angew. Chem., Int. Ed. Engl.* **1988**, *27*, 89−112. (b) Cram, D. J. *Angew. Chem., Int. Ed. Engl.* **1988**, *27*, 1009−1020. (c) Pedersen, C. J. *Angew. Chem., Int. Ed. Engl.* **1988**, *27*, 1021−1027.
(21) (a) Gokel, G. W. *Crown Ethers and Cryptands*; The Royal Society of Chemistry: Cambridge, England, 1991. (b) Lehn, J.-M. *Supramolecular Chemistry*; VCH: Weinheim, 1995. (c) Atwood, J. L.; Davies, J. E. D.; MacNicol, D. D.; Vögtle, F.; Lehn, J.-M.; Gokel, G. W., Eds. *Comprehensive Supramolecular Chemistry*; Pergamon: Oxford, 1996; Vol. 10.
(22) (a) Chang, S.-K.; Cho, I. *J. Chem. Soc., Perkin Trans.* **1986**, 211−214. (b) Olsher, U.; Hankins, M. G.; Kim, T. D.; Bartsch, R. A. *J. Am. Chem. Soc.* **1993**, *115*, 3370−3371. (c) Olsher, U.; Feinberg, H.; Frolow, F.; Shoham, G. *Pure Appl. Chem.* **1996**, *68*, 1195−1199. (d) Danil de Namor, A.; Ng, J. C. Y.; Llosa Tanco, M. A.; Salomon, M. *J. Phys. Chem.* **1996**, *100*, 11485−11491. (e) Arnecke, R.; Böhmer, V.; Cacciapaglia, R.; Dalla Cort, A.; Mandolini, L. *Tetrahedron* **1997**, *53*, 4901−4908. (f) Bartoli, S.; Roelens, S. *J. Am. Chem. Soc.* **1999**, *121*, 11908−11909.
(23) (a) Pederson, C. J. *J. Am. Chem. Soc.* **1970**, *92*, 386−391. (b) Pederson, C. J. *J. Am. Chem. Soc.* **1970**, *92*, 391−394. (c) Burden, I. J.; Coxon, A. C.; Stoddart, J. F.; Wheatley, C. M. *J. Chem. Soc., Perkin Trans.* **1977**, *1*, 220−226. (d) Coxon, A. C.; Stoddart, J. F. *J. Chem. Soc., Perkin Trans.* **1977**, *1*, 767−785. (e) Coxon, A. C.; Laidler, D. A.; Pettman, R. B.; Stoddart, J. F. *J. Am. Chem. Soc.* **1978**, *100*, 8260−8262. (f) Barr, D.; Berrisford, D. J; Mendez, L.; Slawin, A. M. Z.; Snaith, R.; Stoddart, J. F.; Williams, D. J.; Wright, D. S. *Angew. Chem., Int. Ed. Engl.* **1991**, *30*, 82−84. (g) Inoue, I., Gokel, G. W., Eds. *Cation Binding by Macrocycles*; Marcel Dekker: New York, 1990. (h) Deetz, M. J.; Shang, M.; Smith, B. D. *J. Am. Chem. Soc.* **2000**, *122*, 554−562. (i) van de Water, L. G. A.; Driessen, W. L.; Reedijk, J.; Sherrington, D. C. *Eur. J. Inorg. Chem.* **2002**, 221−229.
(24) Marcus, Y. *Chem. Rev.* **1988**, *88*, 1475−1498.
(25) Lindoy, L. F. *The Chemistry of Macrocyclic Ligand Complexes*; Cambridge University Press: Cambridge, 1989.

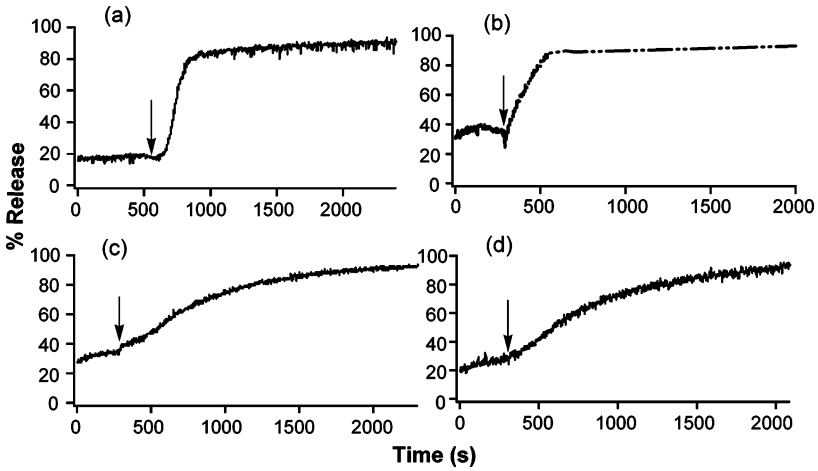


**Figure 7.** Time dependence of the release of coumarin 460 from the naphthyl DB24C8/dialkylammonium nanovalve in $CH_2Cl_2$ caused by 30 $\mu$L of EtOH solution (19 mM) of (a) CsCl, (b) $CaCl_2$, (c) KCl, and (d) LiCl at the time indicated by the arrow.

**Table 1. Properties of the Stimuli and Their Effects on the Controlled Release of Coumarin 460 in Naphthyl Db24C8/Dialkylammonium Nanovalves**

| | organic bases | | | organic salt | | | inorganic salt | | | | |
|---|---|---|---|---|---|---|---|---|---|---|---|
| | HMPT | DIPEA | TEA | $F_2$ DBA | $F_4$ DBA | $(CF_3)_4$ DBA | CsCl | KCl | $CaCl_2$ | LiCl | LiOH |
| size[a]/ionic radius[b] (Å) | 62[a] | 59[a] | 58[a] | | | | 16.7[b] | 13.8[b] | 10.0[b] | 7.6[b] | 7.6[b] |
| binding constant[c] ($M^{-1}$) | | | | 880 ± 220[d] | 790 ± 240[d] | 2900 ± 1200[e] | | | | | |
| half-life $t_{1/2}$ (s) | 450 ± 30 | 300 ± 30 | 100 ± 20 | 400 ± 50 | 500 ± 50 | 440 ± 50 | 130 ± 20 | 380 ± 50 | 100 ± 20 | 450 ± 50 | 330 ± 50 |

[a] By CS Chem3D. [b] Reference 24. [c] The single-site binding constant ($K_a$) is given by $K_a$ = [unfilled site of DB24C8]/([filled site of DB24C8]·[ammonium salt]). [d] With DB24C8 (MeCN, 300 K), refs 11a and 11b. [e] With pyridine-containing [24]crown-8 (MeCN, 298 K, 20 mM), ref 11c.

with DB24C8, despite their large difference in ionic radii.[26] DB24C8 has also been shown[20] to complex with the small cations albeit in a multimetal fashion. A multimetal complexation phenomenon may explain why LiCl causes an observable release. An alternative mechanism could have release caused by ion pairing of $Cl^-$ anion with the ammonium cation to reduce the binding affinity with DB24C8. However, the release rate of the CsCl is much faster than LiCl while the $Cl^-$ concentration is about the same in $CH_2Cl_2$. These results suggest that efficient complexation is more significant than ion pairing to cause a release.

To examine whether a combination of base and metal cation can induce a synergistic effect, the release caused by LiOH (Figure 8a) and LiCl (Figure 8b) were compared. LiCl caused (Figure 8b) a sluggish release with $t_{1/2}$ = 450 ± 50 s, whereas LiOH caused (Figure 8a) a faster release with $t_{1/2}$ = 330 ± 50 s. This observation suggests that the hydroxide ion may participate by deprotonating the ammonium ion. However, since the basicity of the hydroxide ion in $CH_2Cl_2$ is smaller than that of the organic bases, it would not be expected to cause as fast a release.

In pursuit of additional evidence that metal cations open the nanovalves by a competitive binding mechanism, $^1$H NMR spectroscopy was used to monitor the concentration of DB24C8 in the supernatant. The MCM-41 was placed in a quartz cuvette filled with $CD_2Cl_2$ with a total volume of 10 mL. Before the nanovalves were opened, 0.75 mL of the solution was withdrawn and the $^1$H NMR spectrum (Figure 9a) was obtained. After the addition of the CsI/MeOH solution, another 0.75 mL of the solution was withdrawn

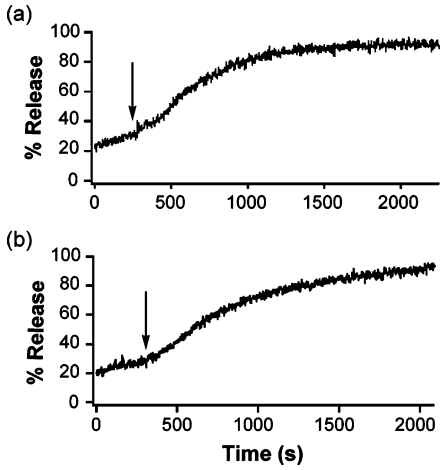


**Figure 8.** Controlled release of coumarin 460 from the naphthyl DB24C8/dialkylammonium nanovalves caused by (a) LiOH and (b) LiCl at the time indicated by the arrows.

and a spectrum recorded (Figure 9b). Prior to activation, low-intensity signals corresponding to the DB24C8 are observed, resulting from DB24C8 that was adsorbed to the silicate surface. The $^1$H NMR spectrum for the solution withdrawn after activation of the nanovalves by CsI shows the presence of DB24C8 signals with much higher intensities, as well as the presence of coumarin 460. The $Cs^+$ cation caused dissociation by the competitive mechanism and the DB24C8/$Cs^+$ complex and the coumarin 460 molecules enter the solution phase. No shift in the DB24C8 $^1$H NMR signals was observed. This unexpected lack of a shift is consistent with a control experiment wherein DB24C8, in $CD_2Cl_2$ in the presence of an excess amount of CsI, exhibits almost identical chemical shifts and intensities as those of pure

(26) Izatt, R. M.; Clark, G. A.; Lamb, J. D.; King, J. E.; Christensen, J. J. *Thermochim. Acta* **1986**, *97*, 115−126.

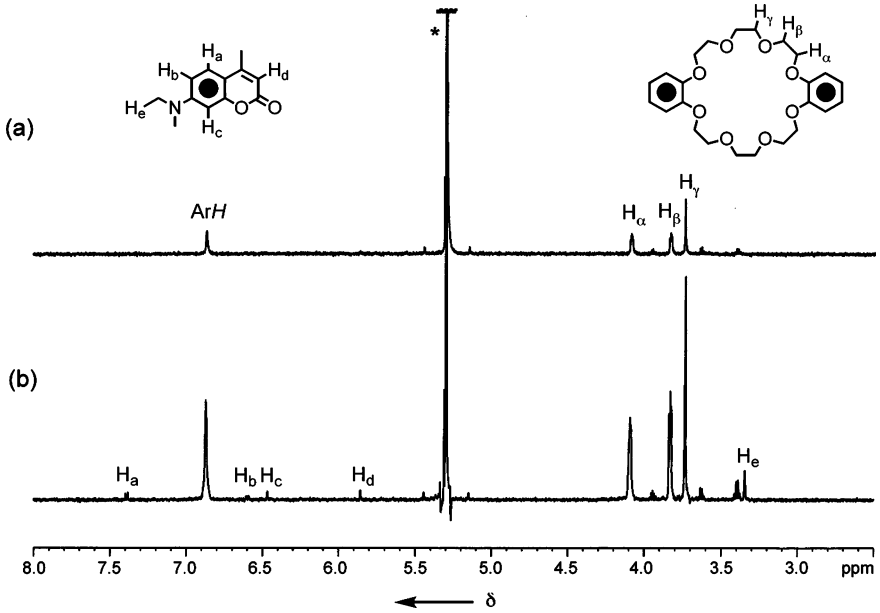


**Figure 9.** $^1$H NMR spectroscopy ($CD_2Cl_2$, 298 K, 500 MHz) is used to monitor the operation of the naphthyl nanovalves. (a) Before controlled release, no coumarin 460 and a small amount of DB24C8 were detected in the solution. (b) After competitive binding driven controlled release of coumarin 460 with CsI, a larger amount of DB24C8 and a small amount of coumarin 460 were detected (∗ = solvent residue).

DB24C8. Thus, the increased DB24C8 and coumarin 460 signals are a result of opening of the nanovalves.

## Summary

The versatility of supramolecular nanovalves based on the controllable DB24C8/dialkylammonium ion recognition motif has been demonstrated through the operation of nanovalves by a wide range of stimuli. In the pH-driven (deprotonation) mechanism, the nanovalves are controlled and their function influenced by the steric bulk of the bases. In the competitive binding mechanism, the nanovalves are operated by intercepting the crown ether with ions that have larger binding affinities such as metal and the fluorodialkylammonium cations. Release of the probe molecules via either deprotonation or competive binding has a half-life ranging from 100 to 500 s. In the case of deprotonation employing different organic bases (tertiary amines), the controlled release is governed by mainly the size as well as the basicity: the rate of release is TEA > DIPEA > HMPT. In the case of the competitive binding employing different organic salts (secondary fluorodialkylammonium salts), where the deprotonation mechanism is not applicable, the release profiles are very sluggish—with half-lives ranging from 400 to 500 s because the organic salts and the tethered dialkylammonium ion have similar binding affinities toward DB24C8. When inorganic salts are employed for the controlled release and a competitive binding mechanism, the half-lives range from 100 to 450 s. In this case, the controlled release depends mainly on the ionic radius of the metal cation employed in the DB24C8 complexation (rate of release: $Cs^+ \sim Ca^{2+} > K^+ > Li^+$) and is also influenced by a counterion effect (rate of release: e.g., $OH^- > Cl^-$ for $Li^+$). These comparative studies carried out on these nanovalves using different bases and salts reveal the ability of these supramolecular systems to respond predictably and selectively to a wide range of stimuli.

**Acknowledgment.** The research was conducted as part of an NSF-NIRT program and DMR 0346601 to J.I.Z. T.D.N. acknowledges the award of a UCLA Dissertation Year Fellowship. The authors thank Cari Pentecost for help in producing graphical representations and Monty Liong for discussions. The powder XRD instrument used in this work was obtained under equipment grant number DMR-0315828.

**Supporting Information Available:** Model studies using phenyl and anthracenyl supramolecular nanovalves, SEM image of silica nanoparticles, various plots of luminescence intensity, and additional experimental procedures. This material is available free of charge via the Internet at http://pubs.acs.org.

CM061682D